大韓土木學會論文集
第14卷 第4號 · 1994年 7月
pp. 827~838

道 路 工 學

반복하중을 받는 입상재료의 회복탄성거동에 관한 구성모델

Constitutive Modeling for Resilient Behavior of Granular Materials under Repeated Loading

이 석 근*
Rhee, Suk Keun

Abstract

Numerous pavement response models rely on constitutive relationships to describe the response of granular materials. In this study, a nonlinear elastic constitutive model which is a function of bulk stress and octahedral shear stress is proposed to describe the resilient behavior of thick granular base courses under flexible airfield pavements. Special features of this model are its accuracy to predict the nonlinear resilient behavior, its simplicity to determine the material constants and its ability to model the secondary effect of decreasing the resilient modulus due to shear effects. In laboratory tests, the nonlinear resilient behavior of granular materials is investigated and values of resilient moduli are determined to provide data for verifying the proposed model. It is found that the resilient modulus is much more dependent on the states of stresses in terms of bulk stress and deviator stress than any other factors. Result of comparison shows that predicted values of resilient moduli are in good agreement with the measured values indicating that the proposed model is suitable to describe the nonlinear resilient behavior of the granular material with wide range of stress states which meet in airfield pavements.

요 지

많은 포장구조 거동 모델은 입상재료의 거동을 묘사하는 구성방정식에 의존하고 있다. 본 연구에서는 비행장 포장의 입상재료 기층의 거동 예측을 위하여, 체적응력(bulk stress)과 팔면체 전단응력(octahedral shear stress)의 함수로 표시된 구성모델이 제안되었다. 이 모델의 특징은 비선형거동을 정확히 예측할 수 있고, 모델상수를 간단히 구할 수 있으며 전단효과에 의한 회복탄성계수의 감소현상을 나타낼 수 있다. 실내시험을 통하여 입상재료의 비선형 회복탄성거동을 관찰하였으며, 제안된 모델을 입증하기 위해 회복탄성계수를 측정하였다. 체적응력과 축차응력이 회복탄성계수의 변화에 가장 주요한 변수임이 관찰되었으며, 실내시험 결과 제안된 모델식에 의한 회복탄성계수의 예측치가 실측치와 잘 일치함을 알 수 있었다. 따라서 제안된 모델식은 비행장 포장에서 일어날 수 있는 광범위한 응력조건하의 입상재료의 회복탄성거동을 잘 묘사할 수 있음을 알 수 있다.

* 정회원 · 한국도로공사 도로연구소 책임연구원

1. Introduction

It is well known that most pavement materials do not respond to traffic loadings in a linearly elastic manner as defined by the theory of elasticity. In recent years, highway engineers have devoted considerable effort to determining the nonlinear stress-strain characteristics of granular materials. Attempts have been made to formulate constitutive models for pavement materials to predict pavement response to loadings, but the stress-strain relations formulated are generally accurate only for a limited range of loadings and boundary conditions.

Particular concern of this study is a flexible airfield pavement constructed with asphalt concrete surface and thick granular base under heavy loadings. The resilient characteristics of untreated granular materials are dependent on the applied stresses. A number of different expressions have been proposed to represent this stress dependency. Among them, two models have been popularly and extensively used to describe the resilient response of granular materials under repeated loadings. The first equation (Eq. 1) expresses the resilient modulus as a function of the applied confining pressure (σ_3), and the second (Eq. 2) expresses the modulus in terms of bulk stress (θ=sum of the principal stresses) as follows.[1,2]

$$M_R = K_1 \sigma_3^{K_2} \tag{1}$$

$$M_R = K_3 \theta^{K_4} \tag{2}$$

where M_R is the resilient modulus which is obtained by dividing a cyclic stress by the recoverable strain and K's are regression parameters.

These models have recently met with criticism due to their inability to model certain type of behavior. The bulk stress model (Eq. 2) generally results in a continually increasing modulus with increasing bulk stress. However, it has been shown that a decreasing modulus is measured with increasing bulk stress if confining pressure is held constant.[3] Moreover, the model has been established from data that used a very limited range of stress paths.

The objectives of this study are to investigate the behavior of granular materials under repeated loading, to identify or develop the nonlinear elastic constitutive relationship which best models the actual stress or recoverable strain states in pavement structures incorporating thick granular layers, and to verify the proposed constitutive model by using laboratory data.

2. Nonlinear Elastic Constitutive Models

Two major categories of constitutive models will be encountered. They are either empirically or theoretically developed models. The theoretically-developed models generally require statistical estimation of parameters using empirical data, while the empirically-developed models rely on empirical results not only for the estimation of parameters but also for formulation of the model itself.

2.1 Bulk Stress Model

One of the most widely used models expresses the resilient modulus as a nonlinear function of the first stress invariant (I_1).[4] This model is primarily empirical in nature and has the form shown in Eq. 3 in which β's are regression parameters.

$$M_R = \beta_1 I_1^{\beta_2} \tag{3}$$

This model has the advantages of simplicity and widespread use. The regression parameters for various granular materials are available in the literature. A comprehensive summary of existing data is presented by Rada and Witczak.[5]

2.2 May and Witczak's Model

May and Witczak[6] found that the deflections predicted by Eq. 3 data did not match field measured deflections due to the shear strain induced in the granular base course by surface loading. They suggested adjustment to the bulk stress model in order to match field measured and predicted values. Since the modulus was found to decrease with increasing shear strain, they suggested the constitutive model of the granular materials should be a function not only of the first stress invariant, but also of the shear strain (ε_{sh}) as follows:

$$M_R = \beta_0 I_1^{\beta_1} f(\varepsilon_{sh}) \quad (4)$$

2.3 Uzan's Model

Extending the work of May and Witczak, Uzan[3] proposed the model as given in Eq. 5 in which σ_d is the deviator stress.

$$M_R = \beta I_1^{\beta_2} \sigma_d^{\beta_d} \quad (5)$$

It is very simple to determine the parameters for this model from most laboratory tests. This model reflects the influence of deviatoric components of the stress tensor. The limitations and disadvantages of this model are similar to those of all empirically based models, i.e., the model has been established from data that used a limited range of stress paths.

In order to accommodate truly triaxial stresses, Eq. 5 can be expressed in terms of the octahedral shear stress, τ_{oct}, instead of the deviatoric stress, σ_d, by using the following relationship.

$$\tau_{oct} = \frac{1}{3}\sqrt{(\sigma_1-\sigma_2)^2+(\sigma_2-\sigma_3)^2+(\sigma_3-\sigma_1)^2} = \frac{\sqrt{2}}{3}\sigma_d \quad (6)$$

Therefore,

$$M_R = \beta_0 I_1^{\beta_1} (\tau_{oct})^{\beta_2} \quad (7)$$

2.4 Lade and Nelson's Model

Lade and Nelson[7] developed a constitutive model which has a good theoretical basis and also has the advantage that it contains explicitly not only the first stress invariant (I_1) but also Poisson's ratio and the second invariant of the deviatoric stress tensor (J_2) as Eq. 8.

$$M_R = \beta_0 P_a \left[\left(\frac{I_1}{P_a}\right)^2 + R\frac{J_2}{P_a^2}\right]^{\beta_1} \quad (8)$$

where P_a is the atmospheric pressure and $R=6(1+\nu)/(1-2\nu)$.

These terms of stress invariants and Poisson's ratio are highly desirable if the model is to adequately consider state of stress. However, in order to be valid, a constant Poisson's ratio must be used for a given stress state because the model derivation assumes a constant value of this parameter.

2.5 Lytton's Model

In order to eliminate the limitation of Lade and Nelson's model which assumes a constant Poisson's ratio, Lytton[8] develop a Poisson's ratio model of the form as Eq. 9.

$$\ln(1+\nu) = b\left(\frac{I_1^2}{3} - J_2\right)^m \quad (9)$$

This Poisson's ratio model is developed theoretically as a function of I_1 and J_2. Lytton proposed a new constitutive equation by replacing Poisson's ratio in the term of R in Eq. 8 by the Poisson's ratio in Eq. 9 which results in the following relationship.

$$\ln(M_R) = a\left[\frac{3-2e^{b\left(\frac{I_1^2}{3}-J_2\right)^m}}{6e^{b\left(\frac{I_1^2}{3}-J_2\right)^m}} I_1^2 + J_2\right]^m \quad (10)$$

where a, b and m are regression parameters.

3. Selection of Constitutive Relationships

The constitutive model could be selected on the basis of statistical analysis of the ability of the model to define the constitutive relationship with a minimum of variance and assessment of the difficulty associated with acquiring the data. The four models, which are Bulk stress model (Eq. 3), Uzan's model with octahedral shear stress (Eq. 7), Lade and Nelson's model (Eq. 8) and Lytton's model (Eq. 10), are chosen in this study to be assessed by various published experimental data sets (Table 1) from repeated load triaxial tests on granular materials.

3.1 Statistics

The results of regression analysis using the above models are summarized in Table 2. Table 2 shows the R^2 and F value of each model for experimental data sets. From Table 2 it is clear that Eq. 7 is superior to the other models.

Considering Eqs. 8 and 10 require additional measurement of radial displacement in the laboratory, Eq. 7 is quite successful in modeling behavior at no increase in laboratory equipment upgrading costs. The subset of this model, which is the bulk stress model, is presently widely used

Table 1. Information of Experimental Data Compiled from Literature

Data Source	Materials	Speimen Size	Data Points	Max. Stress Ratio	Min. Stress Ratio	Unit Wt. (pcf)
Monismith *et al.*[9]	Well Graded Gravel	3.9″ dia. 7.8″ high	18	5	1.5	138.7
Allen[10]	Crushed Limestone & Silicious Gravel	6″ dia. 10″ high	17-19 per each set	10-8.5	2.4-1.5	139.2-129.7
Kalcheff & Hicks[11]	Grey Dolomitic Limestone	6″ dia. 10″ high	37	6	3	143.6
Pappin[12]	Well Graded Crushed Limestone	6″ dia. 12″ high	16	6	1.3	141.4
Cole *et al.*[13]	Crushed Limestone & Gravelly Sand	6″ dia. 10″ high	84	13	1.5	111.4-135.2

and there is a substantial amount of data generated in the development as well as in the use of the model. Also, it is anticipated that modification to existing programs and analytical models which use the bulk stress model to accept the Uzan's model will be minimized. Therefore, in terms of simplicity and economy, Uzan's model seems to be slightly superior.

3.2 Model Generality

When the analysis is to cover a wider range of materials and conditions, more independent variables are required to reflect different specimen conditions. Unit weight (γ) of the granular materials is one of the parameters to be considered in this model generality.

In addition to the unit weight, during the course of this study, it becomes obvious that moisture plays an important role in the behavior of granular material base courses. For analyzing the multiple data sets with different moisture conditions, moisture term must be included among the independent variables. For the gradation typically used in USAF base courses, it seems reasonable to expect that a partially saturated condition will prevail. Therefore, either moisture tension (also called matric suction or potential) and/or moisture content will need to be included in the model. According to Lamborn,[14] the following term should be subtracted from the first stress invariant for the partially saturated condition.

$$3\left(\frac{V_w}{V_t}\right)\psi \tag{11}$$

where V_w/V_t is the volumetric water content and ψ is the suction which has stress unit. Since suction is treated as a negative value, the term in Eq. 11 is added to the first stress invariant of Eq. 7. Therefore, one possible form of the model to be used is given in Eq. 12.

$$M_R=\beta_0(I_1+3\psi\frac{V_w}{V_t})^{\beta_1}(\tau_{oct})^{\beta_2}(\gamma)^{\beta_3} \tag{12}$$

Although very few studies report suction at this time, it has been shown that suction can be related to moisture content (ω) which means that ψ may be replaced with ω in the constitutive equation for certain ranges of suction.[15] Due to the lack of published data on suction, the final form of the model chosen in this study is Eq. 13 to include independent variables for unit weight and moisture content.

Table 2. Results of Regression Analysis of Proposed Models

Data Set	Model	R^2	F
Pappin	Bulk Stress	0.707	33.72
	Uzan	0.988	541.02
	Lade & Nelson	0.927	178.86
	Lytton	0.775	31.98
Monismith	Bulk Stress	0.745	36.76
	Uzan	0.877	53.39
	Lade & Nelson	0.514	16.95
	Lytton	0.594	23.42
Kalcheff & Hicks	Bulk Stess	0.980	1752.54
	Uzan	0.988	1251.66
	Lade & Nelson	0.968	1050.19
	Lytton	0.958	958.40
Cole	Bulk Stress	0.746	248.32
	Uzan	0.872	246.66
	Lade & Nelson	0.793	317.30
	Lytton	0.782	297.37
Allen	Bulk Stress	0.736	44.50
	Uzan	0.954	195.79
	Lade & Nelson	0.925	197.86
	Lytton	0.903	109.60

$$M_R = \beta_0 I_1^{\beta_1} \tau_{oct}^{\beta_2} \gamma^{\beta_3} \omega^{\beta_4} \quad (13)$$

If fixed or constant moisture content is of interest or the model has been developed at certain moisture content, the moisture content term of Eq. 13 may be eliminated.

4. Laboratoty Tests

The repeated load triaxial test is essential to evaluate the resilient modulus of granular base materials. Several researchers have conducted test on granular materials and have provided a comprehensive picture of the influence of various factors such as type and gradation of the aggregate, dry density (void ratio), degree of saturation (moisture content), and magnitude of applied load on resilient modulus.[4,5,16-18] In the laboratory testing program, at least two factors, stress states and moisture content, must be considered. Accordingly several stress states will be induced in the laboratory testing program such as AASHTO T-274 standard, a general guideline for the resilient modulus test.

4.1 Modification of the AASHTO T-274 Test Procedure

In this study, the materials used in the resilient modulus test are specified for Air Force applications. Since the AASHTO standard was designed for highway applications and the contact pressures of truck tires are much lower than those of USAF aircraft,[19] it is necessary to modify the AASHTO standard testing procedure. In order to encompass the desired range of stress states for the base course of the airfield pavement for Air Force applications, the stress combinations of the testing sequence are determined from the result of the triaxial test according to ASTM D3397-81 and employing Mohr-Coulomb failure envelope concept and resulted in higher stress state and stress ratio being applied to the specimen. Although sand material is tested using the standard stress sequence, the stress combinations for the base material are reestablished as shown in Table 3.

4.2 Material and Specimen Preparation

The materials to be tested are a well graded crushed limestone as base and a very uniform fine beach sand as subbase supplied by Tyndall Air Force Base (AFB). The details of the properties of these two materials are summarized in Table 4.

The crushed limestone specimens are 12 inches in length and 6 inches in diameter and are moulded by impact compaction in seven layers with the compaction effort designated CE55 of MIL-STD-621A, Method 100. This compaction effort is the same as that designated by ASTM D1557. In this study, two different moisture contents are used for the base course sample. One is a relatively wet base course in which the moisture content is the same as optimum moisture (4.76%), and the other one is a fairly dry base course in which the moisture content (1%) is the same as

Table 3. The Proposed Stress State and Sequence for the Base Material

Confining Pressure (psi)	Deviator Stress (psi)	Stress Ratio (σ_3/σ_1)
30	75	2.5
	120	4
	180	6
	270	9
20	40	2
	60	3
	80	4
	120	6
	180	9
10	20	2
	30	3
	40	4
	60	6
	90	9
5	10	2
	15	3
	20	4
	30	6
	45	9
1	6	6
	9	9
	14	14
	17	17
	24	24

that measured in the field at Tyndall AFB.

Since the uniform sand is not suitable for impact compaction, a vibrating compaction method is used. The sand is compacted in five layers using a vibratory table in accordance with ASTM D4253. For the subbase material, two different moisture contents are used. These include the moisture content (14.3%) at the depth near Multi-Depth Deflectometer anchor and the field moisture content (3.8%) at the depth near the upper part of the subbase layer.

4.3 Deformation Measurement

Axial deformation is measured by three linear

Table 4. Properties of the Base and Subbase Materials

Properties	Crushed Limestone for Base	Sand for Subbase
Apparent specific gravity	2.68	2.655
Uniformity coeficient	10.7	1.85
Coefficient of curvature	1.37	0.96
Plastic index	NP	NP
AASHTO classification	A-1-a	A-3
Unified classification	GW	SP
Optimum moisture content (%)	4.76	–
Maximum dry density (pcf)	140.8	–
Minimum index density (pcf)	–	85.3
Maximum index density (pcf)	–	102.19

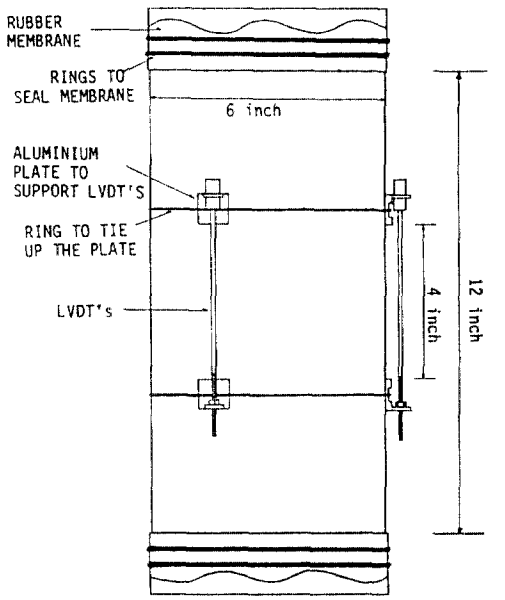

Fig. 1. Side View of Setup for Vertical Displacement Measurement

variable differential transformers (LVDT's) with 0.1 inch full scale linear range, which are equally spaced around the circumference of the specimen as shown in Fig. 1. A 4 inch gauge length is used to minimize significant errors due to the interaction between the platen and the specimen.[20]

Three radial displacement non-contact transducers are used for radial deformation as shown in

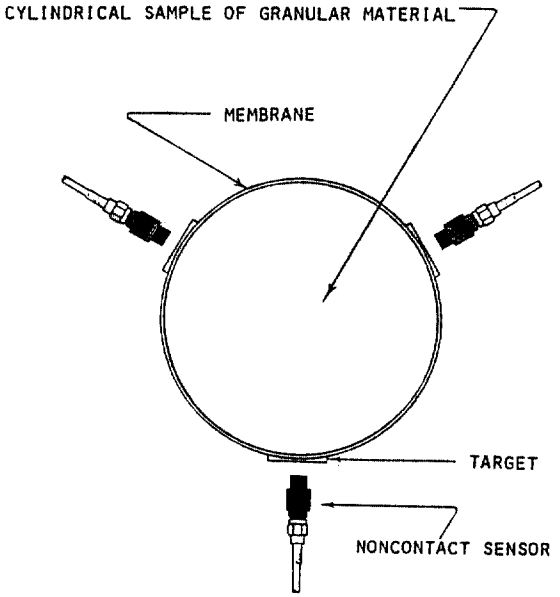

Fig. 2. Top View of Setup for Radial Displacement Measurement

Fig. 2. Radial deformation is measured by detecting the relative movement between the radial transducers and the circular aluminum targets which are anchored at the middle of the specimen. The non-contact transducers are calibrated to function with non-magnetic aluminum targets at 0.02 inch offset and 0.1 inch full scale displacement.

5. Experimental Results of Resilient Modulus Test

Followings are the results of resilient modulus tests of dry and wet samples of base and subbase materials.

5.1 Base Material

The resilient modulus tests are conducted with wide range of principal stress ratio. The influence of applied stresses on the resilient modulus for base materials is shown in Figs. 3 to 5. Fig. 3 shows the effect of confining pressure on the resilient modulus for the dry and wet base material and indicates that the resilient modulus increases with increasing the confining pressure. However, the axial stress also influences on the modulus. At the same confining pressure, the resilient modulus varies with varying the axial stress. The effect of the axial stress (or principal stress ratio)

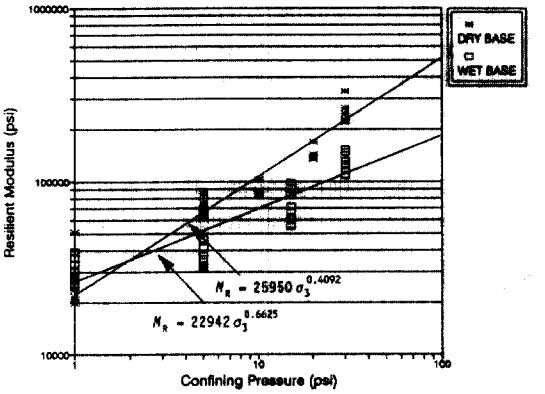

Fig. 3. Variation of M_R with Confining Pressure for Base Material

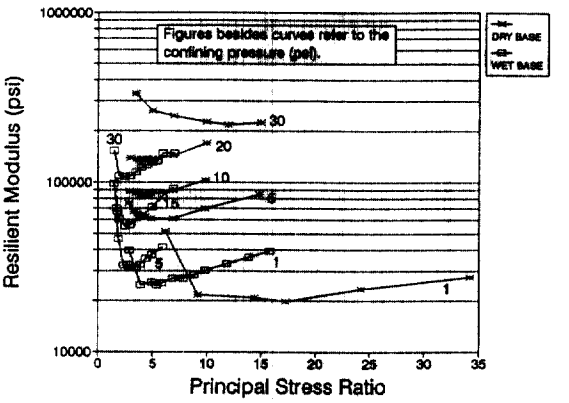

Fig. 4. Variation of M_R with Principal Stress Ratio for Base Material

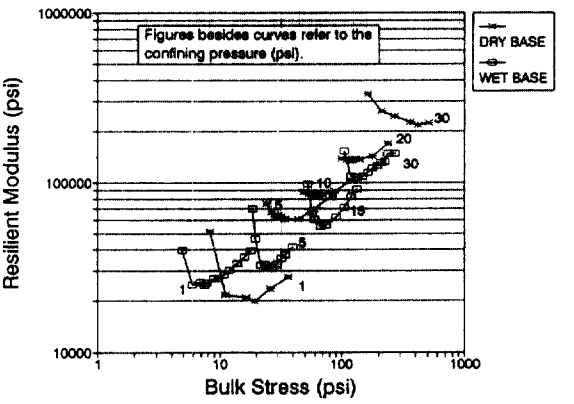

Fig. 5. Variation of M_R with Bulk Stress for Base Material

on the resilient modulus is clearly seen in Fig. 4. This figure shows that the resilient modulus increases with increasing confining pressure at a constant stress ratio. The trend of decreasing the resilient modulus at constant confining pressure with increasing major principal stress is also observed. However, additional trends are also observed in this study. For principal stress ratios greater than 4.0, there is always an increase in the modulus with increasing axial stress except when the confining pressure is 30 psi for the dry base material. For wet specimens, it is clear that the resilient modulus decreases with increasing axial stress for the ratios less than 3.0 and then always increases with increases in axial stress. When the confining pressure is held constant, the resilient modulus decreases with increasing the deviatoric stress at the lower bound of the deviatoric stresses and increases with increasing the deviatoric stress at higher bound of the deviatoric stresses. This trend continues until failure occurs.

The effect of bulk stress on the modulus is illustrated in Fig. 5. In this figure, the data points for the dry base specimen and the wet one have been plotted to show that the resilient modulus increases with increasing bulk stress and the modulus decreases and then increases with increasing the stress ratio at constant confining pressure. Based on the laboratory studies, the full set of curves of constant confining pressure behavior is shown in Fig. 6. There are three curves with thicker line width and one curve with thinner line width. The essentially linear portion of the thin line is the locus of points that would be proposed for use in the traditional bulk stress model. The set of three curves predicts the response at constant confining pressures. The region to the left of the inflection point is the region where deviatoric stress has an effect on reducing the resilient modulus.

In comparison with the dry base material, the wet base material is relatively softer because the resilient moduli are smaller than those of the dry ones at the same stress states. This fact shows that the moisture condition in the specimen affects the stiffness of the specimen. Under undrained conditions, a lower degree of saturation brings about higher stiffness due to the effects of suction.

5.2 Subbase Material

The effect of the axial stress on the resilient modulus of subbase material is shown in Fig. 7. This figure indicates that the resilient modulus decrease lots with increasing axial stress at low level of axial stress. The resilient modulus decreases until the stress ratio is 4.0 for both dry and wet sample. In case of dry sand, the resilient modulus still decreases slightly with increasing the stress ratio above 4.0 of stress ratio. On the other hand, the resilient modulus of wet sand increases slightly with increasing the stress ratio above 4.0 as in the base material.

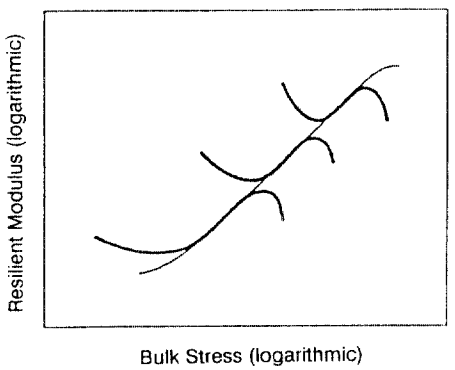

Fig. 6. A Schematic Diagram of Variation of M_R over the Full Range of Stress State for Base Material

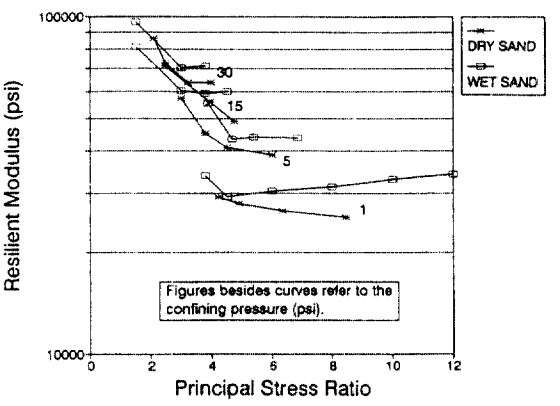

Fig. 7. Variation of M_R with Principal Stress Ratio for Sand

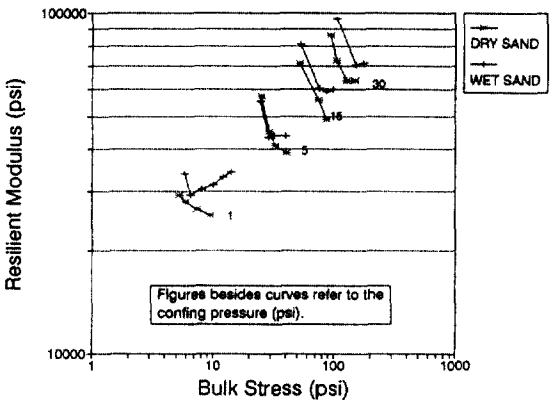

Fig. 8. Variation of M_R with Bulk Stress for Sand

The resilient modulus versus bulk stress for dry and wet sand specimens are shown in Fig. 8. Generally, the resilient modulus increases with increasing bulk stress, but the modulus decreases with increasing bulk stress at constant confining pressure. The wet sand specimen shows that the resilient modulus decreases and then increases with increasing bulk stress at constant confining pressure. This trend is observed in most cases in this study.

6. Comparison of Lab. Measurement With Prediction by the Chosen Model

6.1 Resilient Modulus

Fig. 9 shows comparison of the measured resilient moduli with those predicted by Eq. 13 for the base material. The result of regression analysis is presented in Table 5. From regression analysis, high values of R^2 are obtained and all parameters in the model are significant. This means that predicted values match the measurements very well and the proposed model is suitable to describe the nonlinear resilient behavior of granular material with wide range of stress states which meet in airfield pavements.

The sign of the coefficient of first stress invariant (I_1) in this model is positive and that of octahedral shear stress (τ_{oct}) is negative. The trend of decreasing resilient modulus is due to the effect of τ_{oct} and the trend of increasing resilient modulus is due to the effect of I_1. For the dry

Table 5. Regression Analysis of the Proposed Constitutive Model

Material	Model	R^2
Dry Base	$M_R = 3718\, I_1^{1.1620} \tau_{oct}^{-0.5926}$	0.947
Wet Base	$M_R = 6672\, I_1^{0.6866} \tau_{oct}^{-0.2069}$	0.895
Dry Sand	$M_R = 9728\, I_1^{0.6866} \tau_{oct}^{-0.4734}$	0.976
Wet Sand	$M_R = 12445\, I_1^{0.5854} \tau_{oct}^{-0.3539}$	0.993

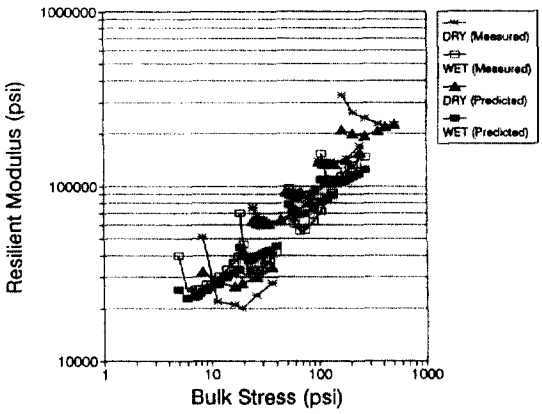

Fig. 9. Measured and Predicted M_R Variation with Bulk Stress for Base Material

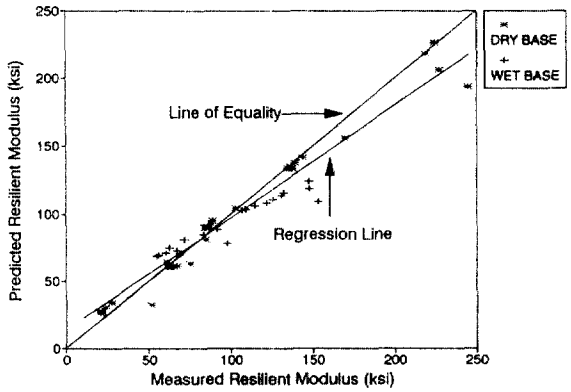

Fig. 10. Comparison of Measured M_R with Prediction for Base Mateiral

material, the predicted M_R by Eq. 13 matches almost perfectly measured M_R at midium range (5 to 20 psi) of confining pressure. In case of wet base material, the modulus predicted by Eq. 13 is still good, and the equation slightly overestimates at midium range (5 to 15 psi) of confining

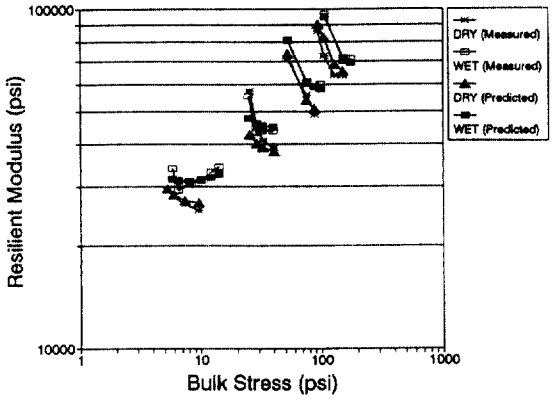

Fig. 11. Measured and Predicted M_R with Bulk Stress for Sand

pressure. The degree of accuracy of the proposed model can be seen in Fig. 10. The model tends to underestimate the resilient modulus at the high level of resilient modulus.

Fig. 11 shows the comparison of measured moduli with prediction for beach sand. It can be seen that the best result is obtained for the wet sand. Since the constitutive model, which is used in evaluation of field data, does not consider the variation of moisture content in a given layer, significant changes in moisture content within a given layer must be approximated by subdividing the original layer into two or more layers that add up to the same thickness as the original layer. Each of the sublayers has different parameters which reflect the change of moisture content with depth.

6.2 Poisson's Ratio

The 'resilient' Poisson's ratio is defined as the ratio of recoverable radial strain (ε_r) to recoverable axial strain (ε_a). This definition can be applied to an ideal isotropic material subjected to a uniform principal stress state. However, laboratory results indicate the granular materials do not behave as an ideal elastic solid because many of measured values of Poisson's ratio are greater than 0.5 due to the anisotropic response nature and dilatancy of the granular material. Therefore, it is desirable to use the 'elastic' Poisson's ratio defined as Eq. 14 from triaxial compression condition, considering the anisotropic response nature

Table 6. Regression Analysis of Poisson's Ratio by Eq. 9

Pisson's Ratio	Materials	R^2	Model Parameters	
			log b (p value)*	m (p value)
'Elastic' Poisson's Ratio (Eq. 14)	Dry Base	0.2741	−0.68684 (0.0001)	−0.03382 (0.0074)
	Wet Base	0.8775	−0.55659 (0.0001)	−0.04664 (0.0001)
	Dry Sand	0.4748	−0.69339 (0.0001)	−0.03497 (0.0045)
	Wet Sand	0.7297	−0.59020 (0.0001)	−0.05527 (0.0001)

*: p value is the level of significance of a statistical test.

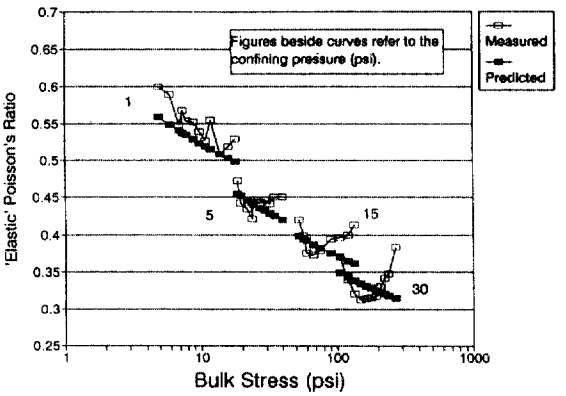

Fig. 12. Measured and Predicted Poisson's Ratio with Bulk Stress for Base Material

and dilatancy of the granular material.

$$\nu = \frac{\sigma_a\varepsilon_r - \sigma_r\varepsilon_a}{[2\sigma_r\varepsilon_r - \varepsilon_a(\sigma_a + \sigma_r)]} \tag{14}$$

where σ_a and σ_r are axial and radial stress, ε_a and ε_r are axial and radial strain, and ν is 'elastic' Poisson's ratio.

The result of the regression analysis of Lytton's model (Eq. 9) for Poisson's ratio on laboratory data is shown in Table 6 which indicates Lytton's model predicts the 'elastic' Poisson's ratio of the wet materials fairly well.

Fig. 12 shows the comparison of measured Poisson's ratio with prediction by Lytton's model for

base course material. As shown in Fig. 12, Poisson's ratio predicted by Eq. 9 decreases with increasing bulk stress under constant confining pressures, and this trend is also observed in the beach sand. Fig. 12 also shows 'elastic' Poisson's ratio decreases with increasing confining pressure and is not sensitive to the stress ratio.

7. Conclusions

The resilient modulus of granular materials is a function of the stress state. It is inadequate to define the stress state only in terms of the first stress invariant. Some explicit form of the deviatoric stress must be included to describe the state of stress more completely.

The resilient modulus of granular materials is more sensitive to stress states than to the degree of saturation. However, for analyzing the multiple data sets in which moisture conditions are different, mositure term must be included among the independent variables.

The final form of the model chosen in this study is given by following:

$$M_R = \beta_0 I_1^{\beta_1} \tau_{oct}^{\beta_2} \gamma^{\beta_3} \omega^{\beta_4}$$

Special features of this model are its accuracy to predict the nonlinear behavior, its simplicity to determine the material constants and its ability to model the secondary effect of decreasing modulus due to shear effects.

Modification to AASHTO T-274 test procedure is necessary to more closely reflect actual states of stress occurred on the airfield pavements.

The behavior of granular material under repeated loading is nonlinear rather than linear. It is found that the resilient modulus is dominantly dependent on the states of stresses in terms of bulk stress and deviator stress. Through the resilient modulus test for the base material and sand, as shown in Fig. 6, the resilient modulus decreases at the lower bound of stress ratio, and then gradually increases until shear failure occurs as increasing the deviator stress under the constant confining pressure.

Another aspect of the resilient modulus test in this study is to use non-contact transducers for radial deformation to measure the Poisson's ratio. Investigation on the Poisson's ratio of granular materials reveals that the Poisson's ratio is somehow dependent on the state of stress and dilative behavior is also observed in the laboratory test. A Poisson's ratio model (Eq. 9) proposed by Lytton, a theoretically developed model, predicts Poisson's ratio fairly well.

The precise determination of the Poisson's ratio of pavement materials is of vital importance in formulating appropriate constitutive relations. For a linear elastic material, it is true that the computed vertical stresses depend very little on the Poisson's ratio, but this does not necessarily mean that the response of the pavement to loads is insensitive to the volume change of the material. In fact, when the constitutive relation of a material is mathematically formulated such as Lytton's model, the modulus of the material depends very much on the manner in which the material changes its volume. Although Lytton's model gives the value of the Poisson's ratio, the model is still subject to the limitations of the testing conditions because material constants in the model must be determined from regression analysis on experimental data.

References

1. H.B. Seed, F.G. Mitry, C.L. Monismith, and C.K. Chan, "Prediction of Flexible Pavement Deflections from Laboratory Repeated Load Tests", NCHRP Report No. 35, HRB, 1967, pp. 118-164.
2. J. Biarez, "Contribution a l'Etude des Properties Mwcaniques des Sols et des Materiau Pulverulents", D.Sc. Thesis, University of Grenoble, France, 1962.
3. J. Uzan, "Characterization of Granular Material", Analysis and Testing of Granular Bases and Subbases, Transportation Research Record 1022, TRB, 1985, pp. 52-59.
4. R.G. Hicks and C.L. Monismith, "Factors Influencing the Resilient Response of Granular Materials", Highway Soils Engineering, Highway Research Record 345, HRB, 1971, pp. 15-31.
5. G. Rada and M.W. Witczak, "Comprehensive Evaluation of Laboratory Resilient Moduli Results for

Granular Material", Layered Pavement System, Transportation Research Record 810, TRB, 1981, pp. 23-33.
6. R.W. May and M.W. Witczak, "Effective Granular Modulus to Model Pavement Responses", Layered Pavement System, Transportation Research Record 810, TRB, 1981, pp. 1-9.
7. P.V. Lade and R.B. Nelson, "Modelling the Elastic Behavior of Granular Materials", *International Journal for Numerical and Analytical Methods in Geomechanics*, Vol. 11, No. 5, September-October 1987, pp. 521-542.
8. R.L. Lytton, "Numerical Methods in Geotechnical Engineering", Class Notes of CVEN 647, Texas A&M University, College Station, 1988.
9. C.L. Monismith, H.B. Seed, F.G. Mitry, and C.K. Chan, "Prediction of Pavement Deflections from Laboratory Tests", Proceedings of the 2nd International Conference on the Structural Design of Asphalt Pavements, Ann Arbor, August 1967, pp. 109-140.
10. J.J. Allen, "The Effects of Non-Constant Lateral Pressure on the Resilient Response of Granular Materials", Ph.D. Thesis, University of Illinois, Urbana, 1973.
11. I.V. Kalcheff and R.G. Hicks, "A Test Procedure for Determining the Resilient Properties of Granular Materials", *Journal of Testing and Evaluation*, ASTM, Vol.1, No. 6, November 1973, pp. 472-479.
12. J.W. Pappin, "Characteristics of Granular Material for Pavement Analysis", Ph.D. Dissertation, University of Nottingham, June 1979.
13. D. Cole, D. Bentley, G. Durell, and T. Johnson, "Resilient Modulus of Freeze-Thaw Affected Granular Soils for Pavement Design and Evaluation", Part 1, Laboratory Tests on Soils from Winchendon, Massachusetts, Test Sections, Report 86-4, 1986.
14. M.J. Lamborn, "A Micromechanical Approach to Modeling Partly Saturated Soils", M.S. Thesis, Texas A&M University, College Station, 1986.
15. K.E. Saxton, W.J. Rawls, J.S. Romberger, and R.I. Papendick, "Estimating Generalized Soil-Water Characteristics from Texture", *Journal of Soil Science Society of America*, Vol. 50, 1986, pp. 1031-1036.
16. H.B. Seed, F.G. Mitry, C.L. Monismith, and C.K. Chan, "Factors Influencing the Resilient Deformations of Untreated Aggregate Base in Two-Layer Pavements Subjected to Repeated Loading", Highway Research Record 190, HRB, 1967, pp. 19-57.
17. B.F. Kallas and J.C. Riley, "Mechanical Properties of Asphalt Pavement Materials", Proceedings of the 2nd International Conference on the Structural Design of Asphalt Pavements, Ann Arbor, August 1967, pp. 713-724.
18. J.J. Allen and M.R. Thompson, "The Resilient Response of Granular Materials Subjected to Time-Dependent Lateral Stresses", Transportation Research Record 510, TRB, 1974, pp. 1-13.
19. J.T. Tielking and F.L. Roberts, "Tire Contact Pressure and Its Effect on Pavement Strains", *Journal of Transportation Engineering*, ASCE, 113(1), 1987, pp. 156-71.
20. H.C. Mayhew, "Resilient Properties of Unbounded Roadbase under Repeated Triaxial Loading", Transport and Road Research Laboratory, Report 1088, 1983.

(接受 : 1994. 3. 10)

APPENDIX

1 in. = 0.0254 m, 1 lbs. = 0.45359 kg, 1 psi = 0.0697 kg/cm^2